

Lawrence Berkeley National Laboratory

LBL Publications

Title

Spontaneous fission of the odd-Z isotope Db255

Permalink

<https://escholarship.org/uc/item/5mm917mq>

Journal

Physical Review C, 110(4)

ISSN

2469-9985

Authors

Pore, JL

Younes, W

Gates, JM

et al.

Publication Date

2024-10-01

DOI

10.1103/physrevc.110.l041301

Peer reviewed

The Spontaneous Fission of the Odd- Z Isotope ^{255}Db

J.L. Pore,¹ W. Younes,¹ J.M. Gates,¹ L.M. Robledo,^{2,3} F.H. Garcia,^{1,*} R. Orford,¹ H.L. Crawford,¹ P. Fallon,¹ J.A. Gooding,^{4,1} M. Kireeff Covo,¹ M. McCarthy,^{4,5} and M.A. Stoyer^{1,6}

¹*Nuclear Science Division, Lawrence Berkeley National Laboratory, Berkeley, CA 94720, USA*

²*Departamento de Física Teórica and CIAFF, Universidad Autónoma de Madrid, E-28049 Madrid, Spain*

³*Center for Computational Simulation, Universidad Politécnica de Madrid,*

Campus de Montegancedo, Bohadilla del Monte, E-28660-Madrid, Spain

⁴*Department of Nuclear Engineering, University of California Berkeley, Berkeley, CA 94720, USA*

⁵*Chemical Sciences Division, Lawrence Berkeley National Laboratory, Berkeley, CA 94720, USA*

⁶*Lawrence Livermore National Laboratory, Livermore CA 94550, USA*

(Dated: October 7, 2024)

Experiments conducted at Lawrence Berkeley National Laboratory’s 88-Inch Cyclotron Facility aimed to produce and study the decay of the previously unobserved isotope ^{255}Db . This isotope was produced in the $^{206}\text{Pb}(^{51}\text{V}, 2n)^{255}\text{Db}$ reaction, separated from unreacted beam material and reaction byproducts with the Berkeley Gas-filled Separator (BGS), and then implanted into a double-sided silicon-strip detector at the BGS focal plane. Decay properties of ^{255}Db were determined from the analysis of Evaporation Residue (EVR)-Fission and EVR- α - α correlations. The properties of this new isotope of dubnium differ dramatically from those of its neighboring Db isotopes. ^{255}Db was found to decay primarily by Spontaneous Fission (SF) with a small α -decay branch, where the average half-life of the observed decays was $t_{1/2} = 2.6^{+0.4}_{-0.3}$ ms. Theoretical calculations were performed using the Wentzel-Kramers-Brillouin (WKB) approximation, with parameters calculated within a self-consistent microscopic approach, to see if these unique properties could be reproduced. A SF half-life estimate is obtained that closely matches the measured value, while simultaneously pointing out the sensitivities that need to be further constrained in future work.

PACS numbers:

Isotopes of SuperHeavy Elements (SHE) boast extraordinary numbers of protons and neutrons and push the boundaries of the nuclear chart and our understanding of nuclear structure. Each newly discovered SHE isotope unveils unique decay properties, offering insights into the specific interactions between the protons and neutrons within its nucleus. These decay characteristics are essential for validating theoretical calculations and deepening our understanding of the cohesive forces at play in these exotic nuclei. Typically, SHE isotopes follow one of two primary decay paths: emission of an α particle or Spontaneous Fission (SF). The choice between these decay modes hinges on the shape of the fission barrier for that specific nucleus, in particular, its height and width [1, 2].

A more robust understanding of the mechanism for SF in the SHE region has potential significant implications. It is needed to comprehend reaction mechanisms and guiding the design of future experiments aimed at synthesizing new SHEs [3–6]. Moreover, this understanding may contribute to our understanding of the origins of heavy elements in the cosmos [7]. Despite the progress made in this area, challenges still persist. Most existing theoretical models are primarily tailored to only describe the “simpler” cases of even-even nuclei [8] and there is limited experimental data available for comparison. Presently, concerted efforts are required to collect more experimental data on accessible SHE. This can pave the way for new theoretical frameworks to be developed, allowing for more robust comparisons and validation. We

report here on the newly-observed and unexpected decay properties of ^{255}Db and discuss comparison to theory for this odd- A SHE.

Assertions regarding the synthesis of ^{255}Db were initially proposed in the mid-1970s by the Joint Institute for Nuclear Research, describing a nucleus with an α -decay half-life of 1.6^{+6}_{-4} seconds [9]. A subsequent claim appeared in a Ph.D. thesis, reporting a single α event with an energy of 9564 keV and a lifetime of 56 ms, along with two fission events having lifetimes of 99 ms and 4 ms, respectively [10]. There is clear disagreement between these two reports. Neither of these observations have been confirmed and ^{255}Db has continued to be regarded as undiscovered within the community. The decay properties of the daughter isotope ^{251}Lr have only been reported recently from its direct production in the $^{50}\text{Ti} + ^{203}\text{Tl}$ reaction, where 24 events were observed [11]. These events were distributed between two α decays with energies of 9210(19) and 9246(19) keV and half-lives of $t_{1/2} = 42^{+42}_{-14}$ ms and $t_{1/2} = 24.4^{+7.0}_{-4.5}$ ms, respectively. Here, the 9246(19) keV transition was assigned as the decay of the $7/2^-$ ground state and the 9210(19) decay was assigned as the decay of the $1/2^-$ isomeric state.

A dedicated study was conducted at Lawrence Berkeley National Laboratory’s (LBNL) 88-inch cyclotron facility to explore the production and decay modes of neutron-deficient Db isotopes. This investigation employed the $^{51}\text{V} + ^{206}\text{Pb}$ fusion-evaporation reaction. A beam of $^{51}\text{V}^{12+}$ ions was produced from natural metal

material in the VENUS (Versatile Electron cyclotron resonance for Nuclear Science) ion source [12, 13] and accelerated with the LBNL 88-inch cyclotron to center of target (E_{COT}) energies ranging from 241 to 253 MeV. The beam impinged upon a rotating-target wheel containing four segments of ^{206}Pb , with an approximate thickness of 0.5 mg/cm^2 , vapor deposited onto $2.1\text{-}\mu\text{m}$ thick titanium backing foils. Produced Db isotopes recoiled into the Berkeley Gas-filled Separator (BGS) [14], for separation from any unreacted beam material and other unwanted reaction by-products, before being implanted into a double-sided silicon-strip detector (DSSD) at the BGS focal plane. Further details of the experimental setup and procedure are given in Ref. [15].

The data were then analyzed to look for EVaporation Residue (EVR)- α_1 - α_2 and EVR-SF correlations in order to identify the decay properties of produced Db isotopes. Here, α_1 and α_2 refer to the time ordered first and second α particles detected in the same pixel of the DSSD following the observation of a potential EVR, respectively. For this study, the selection windows for these correlations were detected-EVR channel numbers between 2500 and 3300, α_1 energy = $7 - 11 \text{ MeV}$, and α_2 energy = $7 - 11 \text{ MeV}$. Additionally, the correlation times of EVR-SF and EVR- α_1 events was constrained to $<10 \text{ s}$, and the correlation time of subsequent α events was capped at $<150 \text{ s}$. The selection of these criteria is discussed in detail in Ref. [15]. The detection efficiency for α decay is approximately 50% and for SF is 100%. From the analysis of these data, it was determined that the isotopes ^{256}Db and ^{255}Db had been produced from the $1n$ and $2n$ exit channels of the $^{51}\text{V} + ^{206}\text{Pb}$ reaction, respectively. The maximum cross-section observed for the production of ^{256}Db was observed to be $\sigma(1n, \text{max}) = 0.49(7) \text{ nb}$ at $E_{COT} = 243(2) \text{ MeV}$, and the maximum cross-section observed for the production of ^{255}Db was observed to be $\sigma(2n, \text{max}) = 0.099(31) \text{ nb}$ at $E_{COT} = 251(2) \text{ MeV}$ [15]. The properties of the observed ^{256}Db decay chains are reported in Ref. [15]. The properties of the isotope ^{255}Db will be discussed here.

In the analysis, three α chains were observed and assigned from the decay of ^{255}Db . The specific details of these decay chains are given in Fig. 1. In decay chain 1, two α particles were observed and assigned as the decay of ^{255}Db followed by the decay of ^{251}Lr . In decay chain 2, two α particles were observed and assigned as the decays of ^{255}Db and ^{247}Md , where the decay of ^{251}Lr was not observed. In decay chain 3, three α particles were observed, assigned as the decays of ^{255}Db , ^{251}Lr , and ^{243}Es , where the decay of ^{247}Md was not observed. Note that the assignment of the 8145 keV transition in decay chain 3 is tentative, as the typical ground state decay of ^{243}Es is $7893(10) \text{ keV}$, and such a high-energy transition has not been previously observed in decay studies of ^{247}Md [17].

The three observed α decays of ^{255}Db have energies of

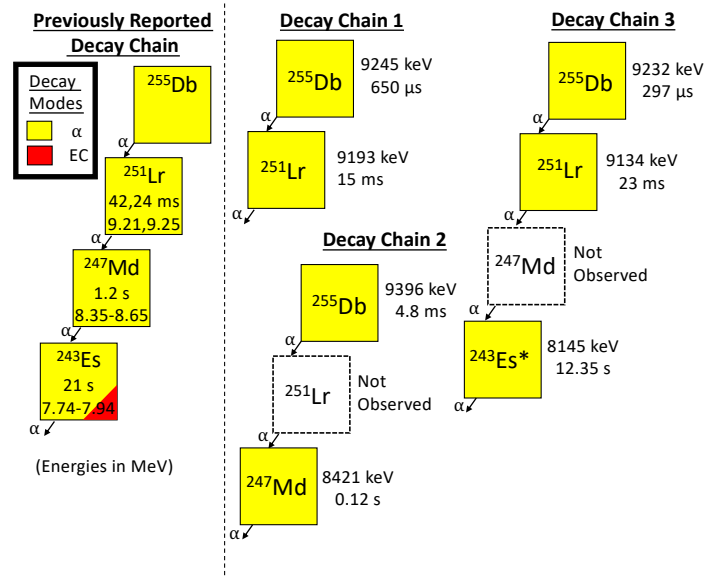


FIG. 1: Previously reported properties of the ^{255}Db decay chain compared to the three α -correlation events observed in this work. Literature values are taken from Refs. [11, 16, 17]. There is a 47 keV error on the detected α energies in the present work.

9245(47), 9396(47), and 9232(47) keV with an average half-life of $t_{1/2} = 1.3^{+1.8}_{-0.5} \text{ ms}$. As was mentioned previously, there have been previous claims as to the production of ^{255}Db where α decay was reported. In Ref. [9], a 1.6^{+6}_{-4} s decay was reported and in the work of Ref. [10] a single 9.5 MeV α was observed with a half-life of 27 ms. Neither of these measurements is in agreement with what has been observed in this study. The properties observed by Ref. [9] are more in line with those of ^{256}Db [18]. However, there could still be the possibility that the properties reported by Ref. [10] could have observed a higher-energy decay of an excited state. The two observed α decays of ^{251}Lr have energies of 9193(47) and 9134(47) keV with correlation times of 15 and 23 ms, respectively. The energies and correlation times of these two events are in line with what was reported previously for ^{251}Lr [11].

The data were also analyzed to look for ^{255}Db SF decays. Potential EVR-SF correlations were identified as is discussed in detail in Ref. [15]. Two clusters of EVR-SF correlations were observed with correlation times $<10 \text{ s}$. The correlation times of these events are plotted in Fig. 2(top). There are 55 events with an average half-life of $2.7^{+0.4}_{-0.3} \text{ ms}$ and 38 events with an average half-life of 1.6^{+3}_{-2} s . The statistics of $\approx 3 \text{ ms}$ SF events and $\approx 2 \text{ s}$ SF events, observed as a function of E_{COT} values, are shown in Fig. 2(bottom). The short-lived SF events were observed primarily at higher E_{COT} values while the longer-lived SF events were primarily observed at lower E_{COT} values, indicating they likely originate from the

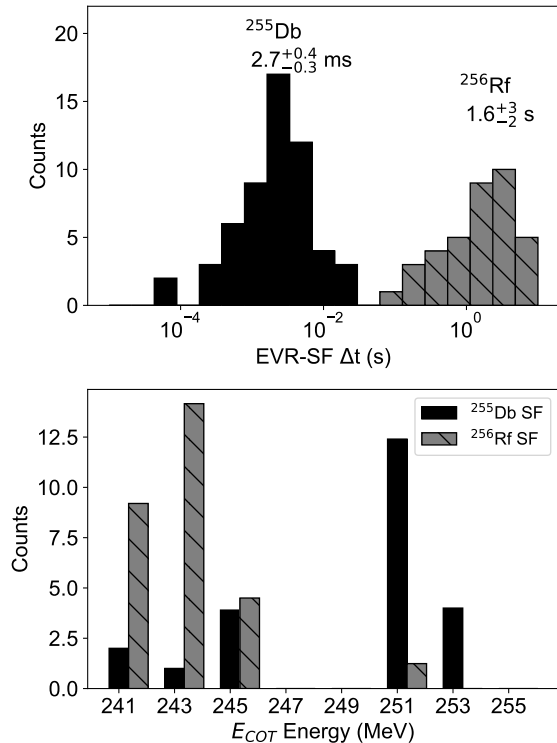


FIG. 2: (Top) The two clusters of observed EVR-SF correlations, assigned as the decays of ^{256}Rf and ^{255}Db , respectively. Note that the correlation times of the ^{256}Rf events also includes the EC decay of ^{256}Db . (Bottom) Distribution of numbers of ^{256}Rf and ^{255}Db SF events. Note that ^{256}Rf SF events are observed primarily at lower E_{COT} and ^{255}Db SF events are observed primarily at higher E_{COT} , indicating that are likely produced from the $1n$ and $2n$ exit channels of the nuclear reaction, respectively.

$2n$ and $1n$ exit channels of the nuclear reaction, respectively. Therefore, the short-lived events are assigned as decays of ^{255}Db and the long-lived events are assigned as the decay of ^{256}Rf , populated via EC of ^{256}Db . Here, the correlation times of the ^{256}Rf events also include the EC decay of ^{256}Db . Such that the total correlation time includes the 1.6 s decay of ^{256}Db [15] and the 6.76 ms decay of ^{256}Rf [19], and would clearly be dominated by the decay of ^{256}Db . Note that a ^{255}Rf SF, populated from the EC decay of ^{255}Db would also have a correlation time of ≈ 1.6 s. However, if ^{255}Rf were to have been populated, it would have decayed with a $\approx 50\%$ α decay branch. No such α decays were observed, therefore the possibility of ^{255}Db undergoing EC was disfavored.

The average half-life of all of the observed ^{255}Db events, including both α and SF decays, is $2.6^{+0.4}_{-0.3}$ ms. Given the level of statistics of α and SF decay events, the decay branches for ^{255}Db are 8(3)% and 92(3)% for α and SF, respectively. These numbers assume a 68% detection efficiency for detecting two α particles within a four- α chain and a 100% detection efficiency for SF

correlations. Here, the α chain detection efficiency was determined assuming that there is a 50% probability that an α event is detected, ^{255}Db underwent α decay, and the α decay branches of the subsequent daughters ^{251}Lr [11], ^{247}Md [16], and ^{243}Es [17].

While neighboring Db isotopes primarily undergo α decay with half-lives on the order of seconds, ^{255}Db exhibits markedly different properties. Previously, predictions for the α and SF half-lives have been performed. Calculations of the α decay half-life were obtained from the Viola-Seaborg-Sobiczewski semi-empirical relation [20, 21], the Coulomb and proximity potential model [22, 23], the universal curve of Poenaru *et al.* [24, 25], the analytical formula of Royer [26], and the Universal decay law of Qi *et al.* [27, 28] and were found to be 1.014 s, 753 ms, 76 ms, 306 ms, and 146 ms, respectively [29]. Considering the 8(3)% α branch observed here, these estimates can be considered to be in agreement with the half-life reported here.

For SF, half-life predictions have varied widely, with reported values of 23.4 s [30], 2.7×10^{-4} s [29, 31], and 9.1×10^{-8} s [32]. Recent calculations, incorporating a generalized liquid drop model and considering nuclear shell effects, have produced estimates ranging from 0.06 to 9.4 s (depending on the choice of the next proton shell closure) [33]. Additionally, existing predictions on the favored decay mode of ^{255}Db are inconsistent, with different studies proposing both α decay and SF as the dominant branch [29–31]. Consequently, the features of ^{255}Db reported here will stand as a crucial reference point for improving theoretical models. These will then be useful for the prediction of SHE decay properties for other isotopes.

In this study, a Wentzel-Kramers-Brillouin (WKB) approximation was adopted within a self-consistent microscopic framework to calculate the SF half-life of ^{255}Db . In this approach, the produced SF half-life relies on calculations of the potential energy and collective mass consistently from nucleons and an effective interaction between them. This internal consistency is important for minimizing uncertainties in the calculation. To further refine the theory and enhance its predictive capability, comparisons to experimental data, such as those presented here are necessary.

As input to the ^{255}Db half-life calculation, Hartree-Fock-Bogoliubov (HFB) calculations using the D1M parameterization of the Gogny interaction were performed [34]. This method treats nucleons as moving independently in a mean-field generated by all other nucleons, and takes into account potential pairing correlations between nucleons. In this instance, to simplify the treatment of the odd proton, as it cannot be easily accommodated in paired states, an Equal Filling Approximation (EFA) was used [35]. This effectively treats the odd proton as if it were distributed equally between the orbitals of a paired state. The exchange part of the Coulomb

repulsion between protons was calculated using a Slater approximation and the mean-field and pairing contributions of the two-body center of mass correction were included.

The calculations were carried out in a deformed harmonic oscillator basis with shells up to $N = 17$, using the two different truncation schemes described in [36] and [37, 38], hereafter referred to as “trunc1” and “trunc2”, respectively, to analyze the convergence. In the case of ^{255}Db , trunc1 resulted in a smaller basis compared to trunc2, such that a comparison between these two schemes can give an indication of the sensitivity of the results compared to the size of the basis. The WKB estimate of the SF half life was obtained using the standard formula [39, 40]

$$T_{1/2}(\text{SF}) = 2.86 \times 10^{-21} (1 + e^{2S}) \text{ sec} \quad (1)$$

with the action integral given by

$$S = \int_a^b dq \sqrt{2B(q) [V(q) - (E_{\min} + E_0)]} \quad (2)$$

and where a and b are the classical turning points, $B(q)$ is the collective mass with respect to coordinate q , $V(q)$ is the HFB-EFA energy modified by the rotational and vibrational zero-point energy (ZPE) corrections, E_{\min} is the minimum of $V(q)$ at the ground-state deformation, and E_0 is a correction to account for quantum fluctuations in the quadrupole moment [39, 40]. In the present work we use $E_0 = 1 \text{ MeV}$. This choice for E_0 has been used in previous calculations [41] as a typical value for SF half-life calculations. As in previous calculations of the SF half lives [38, 42, 43], we have maintained axial symmetry along the fission path, even though the triaxial degree of freedom is known to lower the first barrier by several MeV. We assume that the axially symmetric path is generally favored over the triaxial one based on: 1) previous calculations [44, 45] showing that the lowering of the barrier is compensated by an increase in the collective inertia leading to a larger action integral for the triaxial path, and 2) the ability of pairing fluctuations to restore axial symmetry along the fission path [46, 47].

For the calculations along the fission path, we have followed the approach in Refs. [39, 40] and identified the K quantum number (projection of the angular momentum on the symmetry axis) of the ground state as $K = 9/2$, and assumed that the nucleus maintains this K value all along the fission path. The $K = 9/2$ value was determined through HFB-EFA blocking calculations at the ground state deformation ($Q_{20} = 32 \text{ b}$) as the lowest energy configuration. It should be noted that a $K = 5/2$ configuration was very close in energy to the $K = 9/2$ solution, and could be studied in future sensitivity analyses. The lowest quasiparticle state with $K = 9/2$ has been blocked using the EFA for all HFB calculations along the fission path. In this instance, two different fission paths were calculated, a static path and a dynamic

path. In a static fission path, it is assumed that the nucleus evolves towards the scission point by minimizing its energy, whereas in a dynamic path any potential fluctuations and variations in the relevant collective degrees of freedom of the nucleus that minimize the action as it approaches scission are considered. Note that although the static path is not expected to yield a realistic estimate of the SF half-life, it is useful to include it to show the sensitivity of the half life to the fission path.

The energy and mass curves are plotted in Fig. 3. As shown in Fig. 3(a), the larger basis (trunc2) yields the lower energy curve, and will be used exclusively for the more accurate half-life estimates further below. Fig. 3(b) shows very close agreement between the two truncations schemes. Calculations along the static fission path yield estimates that are much larger than the experimental half-life. The trunc1 basis yields a half-life estimates of $3.2 \times 10^5 \text{ s}$, while the trunc2 basis estimate is 93.8 s . Additionally, note that the trunc2 basis estimates are significantly lower than those from trunc1.

It is expected that a more realistic estimate of the ^{255}Db half-life would come from calculating a dynamic fission path. This requires considering additional relevant collective degrees of freedom explored by the nucleus, such as pairing. The importance of pairing in the description of fission has been previously noted [48–51]. It was shown in Ref. [51] that constraints on collective variables other than pairing have little impact on the dynamic-path results compared to the static-path calculations. We have therefore explored variations in the total particle number (proton and neutron) fluctuation $\Delta N^2 \equiv \langle \hat{N}^2 \rangle - \langle \hat{N} \rangle^2$ around the static solution to allow for dynamical variations in pairing. The proton pairing energies are reduced by the quenching of pairing correlations due to the blocking in the HFB-EFA calculations, as was observed for neutron blocking in ^{243}U in [40].

In practice, this was accomplished by introducing an additional constraining field to the Hamiltonian corresponding to ΔN^2 with a scale parameter λ_2 . The parameter λ_2 is a monotonic function of ΔN^2 and has therefore been used as the collective variable instead of ΔN^2 . As in Ref. [49], we have used a nonperturbative cranking formula to calculate the inertial mass with respect to λ_2 and we have neglected the coupling between Q_{20} and λ_2 . The action-minimizing path in the (Q_{20}, λ_2) space was then determined using a dynamic programming algorithm [52]. The action integral for the static and dynamic paths for the trunc2 calculation are plotted in Fig. 3(c), and it can be seen that the bulk of the contribution to the integrals occurs in the region of the first barrier ($Q_{20} \approx 40 - 100 \text{ b}$). The optimal path lies entirely in the $\lambda_2 > 0$ region, which corresponds to values of ΔN^2 larger than those along the static path.

This result is in keeping with previous observations [50, 51, 53] that the competition between the collective mass

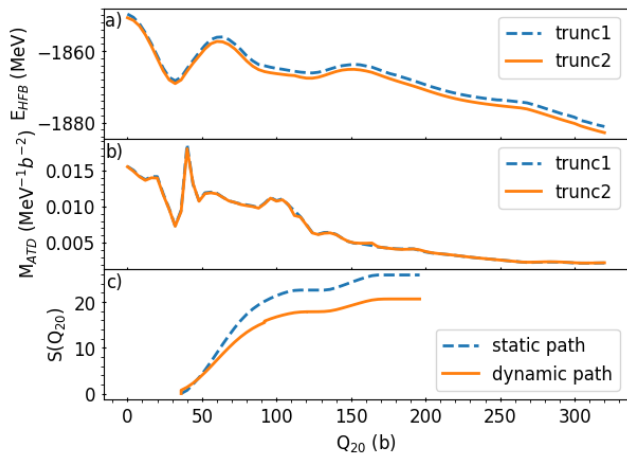


FIG. 3: Comparison of the static-path calculation using the two basis truncation schemes discussed in the text for a) HFB energies and b) Adiabatic Time-Dependent masses with respect to Q_{20} . Panel c) shows the running action integral (Eq. (2)) for trunc2 for both the static and dynamic paths.

(which varies as the inverse square of the pairing gap) and the energy (which varies as the square of the pairing gap) drives the minimum of the action integral toward larger values of the pairing gap compared to the static path. The dynamic-path calculation in the larger basis (trunc2) yields an estimate of the ^{255}Db SF half life of 2.6 ms, in agreement with the present measured value of $2.7_{-0.3}^{+0.4}$ ms. Introducing pairing as a degree of freedom in this calculation brings the half-life prediction down from 93.8 s to a value that is very similar to the one measured experimentally. This surprisingly good agreement must be balanced against the sensitivities of the calculation. In particular a variation in E_0 of just 100 keV changes the estimated half life by a factor of ≈ 3 . It is therefore most prudent to view this result as very promising, while recognizing that further work is needed to constrain the quantities it depends on.

This letter reports the first observation of the production and decay of the isotope ^{255}Db from the $^{51}\text{V} + ^{206}\text{Pb}$ nuclear reaction. Decays via α emission and SF were both observed with a fast average half-life of $2.6_{-0.3}^{+0.4}$ ms. Interestingly, the short half-life and preferred SF decay mode of ^{255}Db differentiate it from its neighboring Db isotopes. These observed properties are of interest for theoretical calculations. A theoretical estimate of the SF half-life was presented from an established microscopic approach that continues to show great promise. In the future, locking down the sensitivities in these calculations, such as the value of the quantum fluctuation correction, will help develop this into a predictive tool for SHE half-lives and decay modes.

ACKNOWLEDGMENTS

We gratefully acknowledge the operations staff of the 88-Inch Cyclotron. This work was supported in part by the U.S. Department of Energy, Office of Science, Office of Nuclear Physics under the contract No. DE-AC02-05CH11231 (LBNL); U.S. Department of Energy, Office of Science, Office of Basic Energy Sciences under contract numbers DE- AC02-05CH11231 (LBNL); The work at Lawrence Livermore National Laboratory is performed under the auspices of the U.S. Department of Energy under Contract DE-AC52-07NA27344 (LLNL); The work of LMR is supported by Spanish Agencia Estatal de Investigacion (AEI) of the Ministry of Science and Innovation under Grant No. PID2021-127890NB-I00.

* Present affiliation: Department of Chemistry, Simon Fraser University, 8888 University Drive, Burnaby, British Columbia, V5A 1S6, Canada

- [1] N. Schunck and D. Regnier, Prog. in Part. and Nucl. Phys. 125, 103963 (2022).
- [2] J. Marin Blanco, A. Dobrowolski, A. Zdeb, and J. Bartel, Phys. Rev. C 108, 044618 (2023).
- [3] M.G. Itkis, G.N. Knyazheva, I.M. Itkis, and E.M. Kozulin, Eur. Phys. J. A 58, 178 (2022).
- [4] S. H. Zhu and Xiao Jun Bao, Phys. Rev. C 108, 014604 (2023).
- [5] R. Zargini and S.A. Seyyedi, Phys. Rev. C 108, 034606 (2023).
- [6] N. Yu. Kurkova and A.V. Karpov, Phys. Atom. Nucl. 86, 311 (2023).
- [7] E.M. Holmbeck, T.M. Sprouse, and M.R. Mumpower, Eur. Phys. J. A 59, 28 (2023).
- [8] M. Kowal, P. Jachimowicz, and A. Sobiczewski, Phys. Rev. C 82, 014303 (2010).
- [9] G.N. Flerov, JINR-E7-10128, (1976)
- [10] A.-P. Leppänen, PhD Thesis, University of Jyv äskylä (Finland) Research Report No. 5/2005 (2005).
- [11] T. Huang et al., Phys. Rev. C 106, L061302 (2022).
- [12] D. Leitner, C.M. Lyneis, T. Loew, D.S. Todd, S. Virostek, and O. Tarvainen, Rev. Sci. Instrum, 77, 03A302 (2006).
- [13] C.M. Lyneis, D. Leitner, M. Leitner, C. Taylor, and S. Abbot, Rev. Sci. Instrum. 81, 02A201 (2010).
- [14] K.E. Gregorich, Nucl. Instrum. Meths. A 711, 47 (2013).
- [15] J.L. Pore, et al., submitted to PRC (2023).
- [16] F.P. Heßberger et al., Eur. Phys. J. A 58, 11 (2022).
- [17] S. Antalic et al., Eur. Phys. J A 43, 35 (2010).
- [18] F.P. Heßberger, et al., Eur. Phys. J. A 12, 57 (2001).
- [19] F.P. Heßberger, et al., Z. Phys. A 359, 415 (1997).
- [20] V.E. Viola Jr., G.T. Seaborg, J. Inorg. Nucl. Chem 28, 741 (1966).
- [21] A. Sobiczewski, Z. Patyk, S. Cwiok, Phys. Lett. B 224, 1 (1989).
- [22] K.P. Santosh, A. Joseph, Pramana 62 957 (2004).
- [23] K.P. Santosh, A. Joseph, Pramana 59 599 (2002).
- [24] D.N. Poenaru, R.A. Gherghescu, W. Greiner, Phys. Rev. C 83, 014601 (2011).
- [25] D.N. Poenaru, R.A. Gherghescu, W. Greiner, Phys. Rev.

- C 85, 034615 (2012).
- [26] G. Royer, *J. Phys. G: Nucl. Part. Phys.* 26, 1149 (2000).
- [27] C. Qi, F.R. Xu, R.J. Liotta, R. Wyss, *Phys. Rev. Lett.* 103, 072501 (2009).
- [28] C. Qi, F.R. Xu, R.J. Liotta, R. Wyss, M.Y. Zhang, C. Asawatangtrakuldee, D. Hu, *Phys. Rev. C* 80, 044326 (2009).
- [29] K. P. Santhosh and C. Nithya, *At. Data and Nucl. Data Tables* 121-122, 216 (2018).
- [30] A. M. Nagaraja, H. C. Manjunatha, N. Sowmya, P. S. Damodara Gupta, and S. Alfred Cecil Raj, *Pram. J. Phys.* 95, 194 (2021).
- [31] K. P. Santhosh and B. Priyanka, *Nucl. Phys. A* 940, 21 (2015).
- [32] Z. Ren and C. Xu, *Nucl. Phys. A* 759, 64 (2005).
- [33] G. Royer, T. Boureau, and N. Potiron, *Phys. Rev. C* 108, 034307 (2023).
- [34] S. Goriely, S. Hilaire, M. Girod and S. Péru, *Phys. Rev. Lett.* 102, 242501 (2009).
- [35] S. Perez-Martin and L. M. Robledo, *Phys. Rev. C* 78, 014304 (2008).
- [36] H. Flocard, P. Quentin, A. K. Kerman, and D. Vautherin, *Nucl. Phys. A* 203, 433 (1973).
- [37] M. Warda, J. L. Egido, L. M. Robledo, and K. Pomorski, *Phys. Rev. C* 66, 014310 (2002).
- [38] S. A. Giuliani and L. M. Robledo, *Phys. Rev. C* 88, 054325 (2013).
- [39] R. Rodríguez-Guzmán and L. M. Robledo, *Eur. Phys. J. A* 52, 348 (2016).
- [40] R. Rodríguez-Guzmán and L. M. Robledo, *Eur. Phys. J. A* 53, 245 (2017).
- [41] R. Rodríguez-Guzmán and L. M. Robledo, *J. Phys. Conf. Ser.* 869, 012061 (2017).
- [42] R. Rodríguez-Guzmán and L. M. Robledo, *Phys. Rev. C* 89, 054310 (2014).
- [43] R. Rodríguez-Guzmán and L. M. Robledo, *Phys. Rev. C* 106, 024335 (2022).
- [44] A. Baran, K. Pomorski, A. Lukasiak, and A. Sobczewski, *Nucl. Phys. A* 361, 83 (1981).
- [45] M. Bender, K. Rutz, P.-G. Reinhard, J. A. Maruhn, and W. Greiner, *Phys. Rev. C* 58, 2126 (1998).
- [46] J. Sadhukhan, J. Dobaczewski, W. Nazarewicz, J. A. Sheikh, and A. Baran, *Phys. Rev. C* 90, 061304(R) (2014).
- [47] J. Sadhukhan, W. Nazarewicz, and N. Schunck, *Phys. Rev. C* 93, 011304(R) (2016).
- [48] A. Staszczak, S. Pilat, and K. Pomorski, *Nucl. Phys. A* 504, 589 (1989).
- [49] J. Zhao, T. Nikšić, and D. Vretenar, *Phys. Rev. C* 104, 044612 (2021).
- [50] R. Rodríguez-Guzmán, L. M. Robledo, C. A. Jiménez-Hoyos, and N. C. Hernández, *Phys. Rev. C* 107, 044307 (2023).
- [51] S. A. Giuliani, L. M. Robledo, and R. Rodríguez-Guzmán, *Phys. Rev. C* 90, 054311 (2014).
- [52] J. Zhao, B.-N. Lu, T. Nikšić, and D. Vretenar, *Phys. Rev. C* 92, 064315 (2015).
- [53] R. Rodríguez-Guzmán and L. M. Robledo, *Phys. Rev. C* 98, 034308 (2018).